Publishing House
AKAPIT

COMPUTER METHODS IN MATERIALS SCIENCE
Informatyka w Technologii Materiałów

Vol. 11, 2011, No. 2

MODELING OF MICROSCALE HEAT TRANSFER IN CYLINDRICAL DOMAINS

BOHDAN MOCHNACKI[1]*, EWA MAJCHRZAK[2]

[1] *Częstochowa University of Technology, Częstochowa, Poland*
[2] *Silesian University of Technology, Gliwice, Poland*
**Corresponding author: bohdan.mochnacki@im.pcz.pl*

Abstract

Thermal processes in a thin metal film subjected to a short-pulse laser heating are considered (axially-symmetrical 2D problem). Heat transfer through thin films subjected to an ultrafast laser pulse is of vital importance in microtechnology applications and it is a reason that the problems connected with a fast heating of solids have become a very active research area.

The heat transfer proceeding in domain analyzed (microscale heat transfer) is described by dual phase lag model (DPLM). According to the newest opinions the DPLM constitutes a very good description of real heat transfer processes proceeding in the micro-scale domains subjected to the strong external heat flux. The base of DPLM formulation is a generalized form of Fourier law (GFL) in which two time parameters τ_q, τ_T appear (the relaxation time and thermalization one, respectively). The acceptation of GFL leads to DPLM equation (Özişik & Tzou, 1994; Smith & Norris, 2003).

In the paper the thermal interactions between external heat source q_b and cylindrical micro-domain are analyzed. The capacity of external heat source (the Neumann boundary condition) is given by function dependent on spatial co-ordinates and time. On the boundary beyond the region of laser action, the no-flux condition is assumed. It should be pointed out that the DPL model requires the adequate transformation of boundary conditions which appear in the typical macro heat conduction models. The initial conditions are also known (initial temperature of domain and initial heating rate).

Numerical model of the process discussed bases on a certain variant of FDM presented with full particulars in Chapter 2.

Key words: microscale heat transfer, laser pulse, finite difference method, numerical simulation

1. INTRODUCTION

DPL model bases on the formulation of generalized Fourier's law, in particular (Chen & Beraun, 2001; Chen et al., 2003; Smith & Norris, 2003; Tamma & Zhou, 1998)

$$\mathbf{q}(r,\, z,\, t+\tau_q) = -\lambda \nabla T(r,\, z,\, t+\tau_T) \qquad (1)$$

where $\mathbf{q}$ [W/m^2] is the heat flux, ∇T [K/m] is the temperature gradient, λ [W/(mK)] is the thermal conductivity, while τ_q, τ_T denote the relaxation and thermalization times, respectively, and $\{r, z\}$ are the geometrical co-ordinates (the axially-symmetrical problem for domain oriented in cylindrical coordinate system is here considered).

Using the Taylor formula the first-order approximation of equation (1) takes a form

$$\mathbf{q}(r,\, z,\, t) + \tau_q \frac{\partial \mathbf{q}(r,\, z,\, t)}{\partial t} = -\lambda \left[\nabla T(r,\, z,\, t) + \tau_T \frac{\partial \nabla T(r,\, z,\, t)}{\partial t} \right] \qquad (2)$$

 ISSN 1641-8581

When formula (2) is combined with the well known energy equation one obtains the following heat conduction equation

$$(r,\, z) \in \Omega: \quad c\left[\frac{\partial T(r,z,t)}{\partial t} + \tau_q \frac{\partial^2 T(r,z,t)}{\partial t^2}\right] =$$

$$\nabla\left[\lambda \nabla T(r,z,t)\right] + \tau_T \frac{\partial \nabla\left[\lambda \nabla T(r,z,t)\right]}{\partial t} \qquad (3)$$

where c [J/(m^{3}K)] is the volumetric specific heat, while

$$\nabla\left[\lambda \nabla T(r,z,t)\right] =$$

$$\frac{1}{r}\frac{\partial}{\partial r}\left[r\lambda \frac{\partial T(r,z,t)}{\partial r}\right] + \frac{\partial}{\partial z}\left[\lambda \frac{\partial T(r,z,t)}{\partial z}\right] \qquad (4)$$

In the paper the interactions between an external heat source q_b and cylindrical micro-domain Ω are analyzed. The domain considered is limited by planes $z = 0$, $z = Z$ and surface $r = R$, additionally r_d corresponds to the radius of beam q_b and the boundary heat flux is assumed in the form (Hector et al., 1992)

$$q_b(r,0,t) = 4\, q_0 \frac{t}{t_p}\left(1 - \frac{t}{t_p}\right)\exp\left(-\frac{r^2}{r_d^2}\right) \qquad (5)$$

where q_0 is the factor corresponding to the maximum incident heat flux and t_p is the exposure time.

On the remaining parts of the boundary the no-flux conditions are taken into account

$$(r,z) \in \Gamma_\infty: \qquad q_b(r,z,t) = 0 \qquad (6)$$

The same condition is given along the axis of cylinder. It should be pointed out that the DPL model requires the transformation of boundary conditions which appear in the typical macro heat conduction models. For example, in the case considered one has

$$(r,z) \in \Gamma: \quad q_b(r,z,t) + \tau_q \frac{\partial q_b(r,z,t)}{\partial t} =$$

$$-\lambda\left[\mathbf{n} \cdot \nabla T(r,z,t) + \tau_T \frac{\partial\left[\mathbf{n} \cdot \nabla T(r,z,t)\right]}{\partial t}\right] \qquad (7)$$

The initial conditions (initial temperature of domain and initial heating rate) are also given

$$t = 0: \quad T(r,z,0) = T_0, \quad \left.\frac{\partial T(r,z,t)}{\partial t}\right|_{t=0} = 0 \qquad (8)$$

where T_0 is the constant initial temperature.

2. NUMERICAL MODEL

At the stage of numerical computations the explicit scheme of finite difference method being a generalized version of algorithm presented by Majchrzak and Mochnacki (2004) and Mochnacki and Suchy (1995) has been used.

At first, a time grid

$$t^0 < t^1 < \ldots < t^{f-2} < t^{f-1} < t^f < \ldots < t^F < \infty \qquad (9)$$

with constant time step Δt is introduced.

A geometrical mesh is shown in figure 1. One can see that the internal nodes close to the external or internal boundaries are located at the distance $0.5h$ or $0.5k$ from the boundary Γ_0 or Γ_∞.

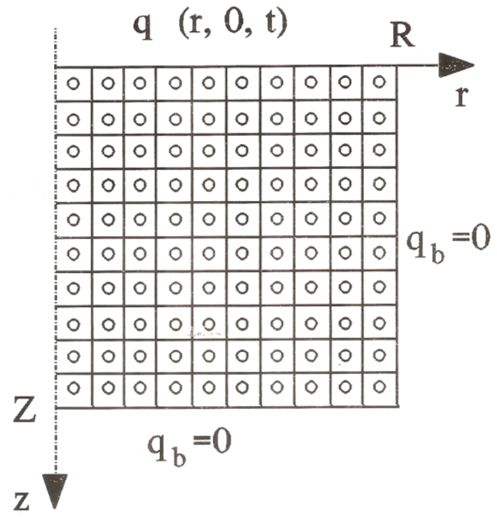

Fig. 1. *Boundary conditions and discretization.*

For transition $t^{f-1} \to t^f$ the following approximation of equation (3) is proposed

$$c\left[\frac{T_{i,j}^f - T_{i,j}^{f-1}}{\Delta t} + \tau_q \frac{T_{i,j}^f - 2T_{i,j}^{f-1} + T_{i,j}^{f-2}}{(\Delta t)^2}\right] =$$

$$\left[\nabla(\lambda \nabla T)\right]_{i,j}^{f-1} + \tau_T \frac{\left[\nabla(\lambda \nabla T)\right]_{i,j}^{f-1} - \left[\nabla(\lambda \nabla T)\right]_{i,j}^{f-2}}{\Delta t} \qquad (10)$$

or

$$\left[\frac{c}{\Delta t}+\frac{c\tau_q}{(\Delta t)^2}\right]T_{i,j}^{f}=\left(1+\frac{\tau_T}{\Delta t}\right)\left[\nabla\left(\lambda\nabla T\right)\right]_{i,j}^{f-1}-$$
$$-\frac{\tau_T}{\Delta t}\left[\nabla\left(\lambda\nabla T\right)\right]_{i,j}^{f-2}+\left[\frac{c}{\Delta t}+\frac{2c\tau_q}{(\Delta t)^2}\right]T_{i,j}^{f-1}-\frac{c\tau_q}{(\Delta t)^2}T_{i,j}^{f-2} \tag{11}$$

where: $T_{i,j}^{f}=T(r_i,z_j,t^f)$, $T_{i,j}^{f-1}=T(r_i,z_j,t^{f-1})$, $T_{i,j}^{f-2}=T(r_i,z_j,t^{f-2})$.

Now, the approximation of the expression $\nabla(\lambda\nabla T)$

$$\left[\nabla\left(\lambda\nabla T\right)\right]_{i,j}^{s}=\left[\frac{1}{r}\frac{\partial}{\partial r}\left(r\lambda\frac{\partial T}{\partial r}\right)\right]_{i,j}^{s}+\left[\frac{\partial}{\partial z}\left(\lambda\frac{\partial T}{\partial z}\right)\right]_{i,j}^{s} \tag{12}$$

where $s=f-1$ or $s=f-2$ will be discussed.

We shall seek the differential analogue of this formula for a 5-point star as shown in figure 2. Let us assume here that the node (r_i, z_j) is the central node, grid step in the direction of r axis is h, and in the direction of z axis is k.

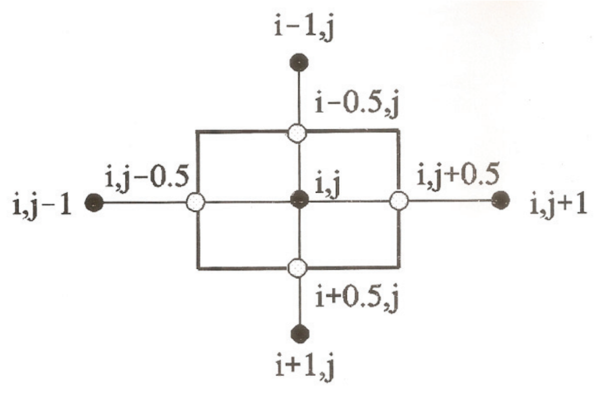

***Fig. 2.** 5-point star.*

At the distances $0.5h$ and $0.5k$ on the arms of the star, auxiliary points were distinguished. We shall make use of the approximation of a derivative by mean quotient. Thus (Mochnacki & Suchy, 1995)

$$\left(r\lambda\frac{\partial T}{\partial r}\right)_{i,j+0.5}^{s}=r_{i,j+0.5}\lambda_{i,j+0.5}^{s}\frac{T_{i,j+1}^{s}-T_{i,j}^{s}}{h}=$$
$$\left(r_{i,j}+\frac{h}{2}\right)\frac{T_{i,j+1}^{s}-T_{i,j}^{s}}{R_{i,j+1}^{s}} \tag{13}$$

$$\left(r\lambda\frac{\partial T}{\partial r}\right)_{i,j-0.5}^{s}=r_{i,j-0.5}\lambda_{i,j-0.5}^{s}\frac{T_{i,j}^{s}-T_{i,j-}^{s}}{h}=$$
$$\left(r_{i,j}-\frac{h}{2}\right)\frac{T_{i,j}^{s}-T_{i,j-1}^{s}}{R_{i-1,j}^{s}} \tag{14}$$

where the conductivities $\lambda_{i,j+0.5}^{s}$ and $\lambda_{i,j-0.5}^{s}$ are approximated by the mean harmonics of the conductivities in the star nodes, namely

$$\lambda_{i,j+0.5}^{s}=\frac{2\lambda_{i,j}^{s}\lambda_{i,j+1}^{s}}{\lambda_{i,j}^{s}+\lambda_{i,j+1}^{s}},\quad \lambda_{i,j-0.5}^{s}=\frac{2\lambda_{i,j}^{s}\lambda_{i,j-1}^{s}}{\lambda_{i,j}^{s}+\lambda_{i,j-1}^{s}} \tag{15}$$

and then

$$R_{i,j+1}^{s}=\frac{0.5h}{\lambda_{i,j}^{s}}+\frac{0.5h}{\lambda_{i,j+1}^{s}},\quad R_{i,j-1}^{s}=\frac{0.5h}{\lambda_{i,j}^{s}}+\frac{0.5h}{\lambda_{i,j-1}^{s}} \tag{16}$$

are the thermal resistances from the node i, j to the nodes $i, j+1$ and $i, j-1$.

We shall still make use of the mean differential quotient. So

$$\left[\frac{1}{r}\frac{\partial}{\partial r}\left(r\lambda\frac{\partial T}{\partial r}\right)\right]_{i,j}^{s}=$$
$$\frac{1}{r_{i,j}h}\left[\left(r_{i,j}+\frac{h}{2}\right)\frac{T_{i,j+1}^{s}-T_{i,j}^{s}}{R_{i,j+1}^{s}}+\left(r_{i,j}-\frac{h}{2}\right)\frac{T_{i,j-1}^{s}-T_{i,j}^{s}}{R_{i,j-1}^{s}}\right] \tag{17}$$

In similar way one obtains

$$\left(\lambda\frac{\partial T}{\partial z}\right)_{i+0.5,j}^{s}=\lambda_{i+0.5,j}^{s}\frac{T_{i+1,j}^{s}-T_{i,j}^{s}}{k}=\frac{T_{i+1,j}^{s}-T_{i,j}^{s}}{R_{i+1,j}^{s}} \tag{18}$$

$$\left(\lambda\frac{\partial T}{\partial z}\right)_{i-0.5,j}^{s}=\lambda_{i-0.5,j}^{s}\frac{T_{i,j}^{s}-T_{i-1,j}^{s}}{k}=\frac{T_{i,j}^{s}-T_{i-1,j}^{s}}{R_{i-1,j}^{s}} \tag{19}$$

and next

$$\left[\frac{\partial}{\partial z}\left(\lambda\frac{\partial T}{\partial z}\right)\right]_{i,j}^{s}=\frac{1}{k}\left[\frac{T_{i+1,j}^{s}-T_{i,j}^{s}}{R_{i+1,j}^{s}}+\frac{T_{i-1,j}^{s}-T_{i,j}^{s}}{R_{i-1,j}^{s}}\right] \tag{20}$$

where

$$R_{i+1,j}^{s}=\frac{0.5k}{\lambda_{i,j}^{s}}+\frac{0.5k}{\lambda_{i+1,j}^{s}},\quad R_{i-1,j}^{s}=\frac{0.5k}{\lambda_{i,j}^{s}}+\frac{0.5k}{\lambda_{i-1,j}^{s}} \tag{21}$$

are the thermal resistances from the node i, j to the nodes $i+1, j$ and $i-1, j$.

Finally

$$\left[\nabla\left(\lambda\nabla T\right)\right]_{i,j}^{s}=\frac{\Phi_{i,j-1}}{R_{i,j-1}^{s}}\left(T_{i,j-1}^{s}-T_{i,j}^{s}\right)+$$
$$\frac{\Phi_{i,j+1}}{R_{i,j+1}^{s}}\left(T_{i,j+1}^{s}-T_{i,j}^{s}\right)+\frac{\Phi_{i-1,j}}{R_{i-1,j}^{s}}\left(T_{i-1,j}^{s}-T_{i,j}^{s}\right)+$$
$$\frac{\Phi_{i+1,j}}{R_{i+1,j}^{s}}\left(T_{i+1,j}^{s}-T_{i,j}^{s}\right) \tag{22}$$

where

$$\Phi_{i,j-1}=\frac{r_{i,j}-0.5h}{r_{i,j}h},\quad \Phi_{i,j+1}=\frac{r_{i,j}+0.5h}{r_{i,j}h},$$
$$\Phi_{i-1,j}=\Phi_{i+1,j}=\frac{1}{k} \tag{23}$$

Now, the problem of boundary conditions addition should be explained. In figure 3 a fragment of a rectangular differential grid is shown, in which the node i,j is a 'boundary' one.

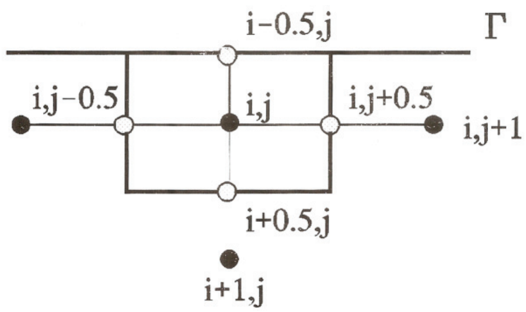

Fig. 3. *Approximation of the 2nd type boundary condition.*

As it was mentioned previously, on the boundary Γ ($z=0$) the condition of the form (5) is assumed, this means (c.f. equation (7))

$$q_b(r,0,t)+\tau_q\frac{\partial q_b(r,0,t)}{\partial t}=$$
$$-\lambda\left[\frac{\partial T(r,z,t)}{\partial z}+\tau_T\frac{\partial^2 T(r,z,t)}{\partial t\partial z}\right]_{z=0} \tag{24}$$

The following approximation of (24) at the point i,j for time t^s can be taken into account

$$\left(q_b\right)_{i-0.5,j}^{s}+\tau_q\left(\frac{\partial q_b}{\partial t}\right)_{i-0.5,j}^{s}=$$
$$-\left(\lambda\frac{\partial T}{\partial z}\right)_{i-0.5,j}^{s}-\frac{\tau_T}{\Delta t}\left[\left(\lambda\frac{\partial T}{\partial z}\right)_{i-0.5,j}^{s}-\left(\lambda\frac{\partial T}{\partial z}\right)_{i-0.5,j}^{s-1}\right]$$
$$\tag{25}$$

or

$$-\left(\lambda\frac{\partial T}{\partial z}\right)_{i-0.5,j}^{s}=$$
$$\frac{\Delta t}{\Delta t+\tau_T}\left[\left(q_b\right)_{i-0.5,j}^{s}+\tau_q\left(\frac{\partial q_b}{\partial t}\right)_{i-0.5,j}^{s}\right]-$$
$$\frac{\tau_T}{\Delta t+\tau_T}\left(\lambda\frac{\partial T}{\partial z}\right)_{i-0.5,j}^{s-1} \tag{26}$$

The aim of our considerations is to find a numerical approximation of the operator $\nabla(\lambda\nabla T)$ at the boundary point i,j for time t^s (c.f. equation (4))

$$\left[\nabla\left(\lambda\nabla T\right)\right]_{i,j}^{s}=\frac{\Phi_{i,j-1}}{R_{i,j-1}^{s}}\left(T_{i,j-1}^{s}-T_{i,j}^{s}\right)+$$
$$\frac{1}{k}\left[\left(\lambda\frac{\partial T}{\partial z}\right)_{i+0.5,j}^{s}-\left(\lambda\frac{\partial T}{\partial z}\right)_{i-0.5,j}^{s}\right] \tag{27}$$

Putting (18) and (26) into (27) one has

$$\left[\nabla\left(\lambda\nabla T\right)\right]_{i,j}^{s}=\frac{\Phi_{i,j-1}}{R_{i,j-1}^{s}}\left(T_{i,j-1}^{s}-T_{i,j}^{s}\right)+$$
$$\frac{\Phi_{i+1,j}}{R_{i+1,j}^{s}}\left(T_{i+1,j}^{s}-T_{i,j}^{s}\right)+$$
$$\Phi_{i-1,j}\frac{\Delta t}{\Delta t+\tau_T}\left[\left(q_b\right)_{i-0.5,j}^{s}+\tau_q\left(\frac{\partial q_b}{\partial t}\right)_{i-0.5,j}^{s}\right]-$$
$$\Phi_{i-1,j}\frac{\tau_T}{\Delta t+\tau_T}\lambda_{i,j}^{s-1}\frac{T_{i+1,j}^{s-1}-T_{i,j}^{s-1}}{k} \tag{28}$$

In similar way the boundary condition ($q_b=0$) on the remaining parts of the boundary (plane $z=Z$ and surface $r=R$) is introduced to the operator $[\nabla(\lambda\nabla T)]^s_{i,j}$.

Finally, the temperature $T_{i,j}^{f}$ at the node i,j for time t^f is calculated using the formula (c.f. equation (11))

$$T_{i,j}^{f}=\frac{\Delta t\left(\Delta t+\tau_T\right)}{c\left(\Delta t+\tau_q\right)}\left[\nabla\left(\lambda\nabla T\right)\right]_{i,j}^{f-1}-$$
$$\frac{\tau_T\Delta t}{c\left(\Delta t+\tau_q\right)}\left[\nabla\left(\lambda\nabla T\right)\right]_{i,j}^{f-2}+\frac{\Delta t+2\tau_q}{\Delta t+\tau_q}T_{i,j}^{f-1}-$$
$$\frac{\tau_q}{\Delta t+\tau_q}T_{i,j}^{f-2} \tag{29}$$

We shall now formulate a criterion of stability of the explicit differential scheme. The solving system constructed on the basis of the explicit scheme is stable if the coefficients in the difference equations for time t^{f-1} are non-negative. Hence it results that the following coefficient must be positive

$$\frac{\Delta t+2\tau_q}{\Delta t+\tau_q}-\frac{\Delta t\left(\Delta t+\tau_T\right)}{c\left(\Delta t+\tau_q\right)}\left[\frac{\Phi_{i,j-1}}{R^{f-1}_{i,j-1}}+\frac{\Phi_{i,j+1}}{R^{f-1}_{i,j+1}}+\frac{\Phi_{i-1,j}}{R^{f-1}_{i-1,j}}+\frac{\Phi_{i+1,j}}{R^{f-1}_{i+1,j}}\right]\geq 0 \tag{30}$$

(the remaining ones are always positive). The inequality (30) allows one to determine the proper time step Δt.

3. RESULTS OF COMPUTATIONS

The example of numerical simulation concerns the heating of microscale cylindrical domain $Z = 100$ nm, $R = 100$ nm, $r_d = 50$ nm subjected to a strong external heat source ($q_0 = 9.59\cdot10^{12}$ W/m^2, $t_p = 100$ fs). Thermophysical parameters of material (chromium) have been taken from Majchrzak et al. (2009a). In figure 4 the example of solution obtained, in particular the temperature field for time $t = 100$ ps (upper part of domain) under the assumption that the initial temperature of domain equals 27°C is shown. Figure 5 illustrates the temperature history at the points corresponding to $r = 0$ and $z = 2.5$ nm (1), $z = 7.5$ nm (2), $z = 12.5$ nm (3), respectively.

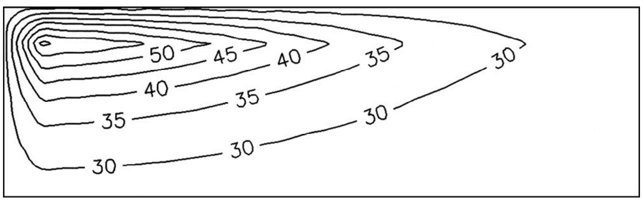

Fig. 4. Temperature distribution for time t = 100 ps.

4. CONCLUSIONS

In the papers presented by Majchrzak et al. (2009a; 2009b; 2009c) the problems close to the problem discussed here are considered, but the thin film oriented in Cartesian co-ordinate system (1D task) is substituted by the 2D object oriented in cylindrical co-ordinates (it results from the assumptions concerning the boundary heat flux). Additionally the solutions presented previously have been obtained under the assumption that the action of external heat flux is taken into account by introduction of internal heat source appearing in the energy equation (e.g. Chen, & Beraun, 2001), while in this paper the interaction between external heat flux and metal film results directly from the boundary condition given for $z = 0$. The change of object geometry and the change of boundary conditions modeling are connected with the essential complications at the stage of numerical algorithm construction.

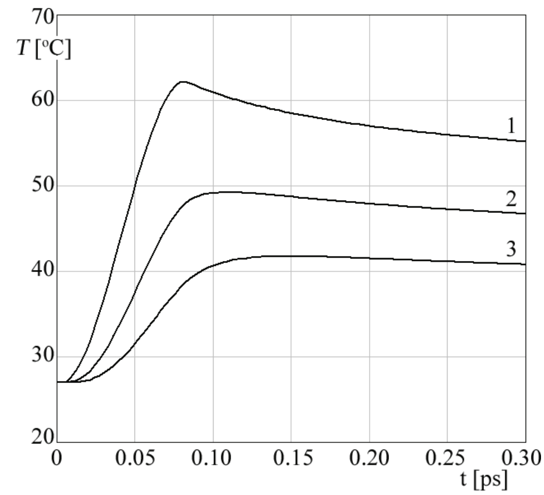

Fig. 5. Temperature history at the points 1 (0, 2.5), 2 (0, 7.5), 3 (0, 12.5).

In the paper the classical variant of FDM for regular geometrical meshes is applied and it can be substituted by the generalized version of this method (e.g. Mochnacki & Majchrzak, 2010). It should be pointed out that the GFDM algorithm which was repeatedly verified as an effective tool of numerical solution of macroscopic heat transfer problems (described by the Fourier equation) was not till now used in the case of microscale heat transfer and the application of GFDM in this field requires the additional scientific researches..

The computer program worked out by authors allows one to consider directly the course of thermal processes both in the case of DPL model and Cattaneo-Vernotte or Fourier ones. The multi-layer domains can be also considered. It is possible to generalize the algorithm on the case of cyclic external heating.

ACKNOWLEDGEMENT

This work was supported by Grant No N N501 2167 37 from the Polish Ministry of Science and Higher Education.

REFERENCES

Chen, J.K., Beraun, J.E., 2001, Numerical study of ultrashort laser pulse interactions with metal films, *Numerical Heat Transfer*, Part A, 40, 1-20

Chen, G., Borca-Tasciuc, D., Yang, R.G., 2004, *Nanoscale heat transfer*, Encyclopedia of Nanoscience and Nanotechnology, X, 1-30.

Majchrzak, E., Mochnacki, B., 2004, *Numerical methods. Theory, numerical aspects, algorithms*, Publication of the Silesian University of Technology, Gliwice, (in Polish).

Majchrzak, E., Mochnacki, B., Greer, A.L., Suchy, J.S., 2009a, Numerical modeling of short pulse laser interactions with multi-layered metal films, *Computer Modelling in Engineering and Sciences*, 41 (2), 131-146.

Majchrzak, E., Mochnacki, B., Suchy, J.S., 2009b, Finite difference model of short-pulse laser interactions with thin metal film, *Computer Methods in Materials Science*, 9 (2), 316-322.

Majchrzak, E., Mochnacki, B., Poteralska, J., 2009c, One-shot' identification of laser intensity in a process of thin metal film heating, *Scientific Research of the Institute of Mathematics and Computer Science*, Czestochowa University of Technology, 1(8), 131-136.

Mochnacki, B., Suchy, J.S., 1995, *Numerical methods in computations of foundry processes*, Polish Foundrymen's Technical Association, Cracow.

Mochnacki, B., Majchrzak, E., 2010, Numerical modeling of casting solidification using generalized finite difference method, *Materials Science Forum*, 638-642, 2676-2681.

Özişik, O., Tzou, D.Y., 1994, On the wave theory in heat conduction, *Journal of Heat Transfer*, 116, 526-535.

Smith, A.N., Norris, P.M., 2003, *Microscale heat transfer*, Chapter 18 in: Heat Transfer Handbook, John Willey&Sons.

Tamma, K.K., Zhou, X., 1998, Macroscale and microscale thermal transport and thermo-mechanical interactions: some noteworthy perspectives, *Journal of Thermal Stresses*, 405-449.

MODELOWANIE MIKROSKALOWEGO PRZEPŁYWU CIEPŁA W OBSZARACH CYLINDRYCZNYCH

Streszczenie

W pracy rozpatruje się proces przepływu ciepła w mikroobszarach poddanych działaniu wiązki laserowej (zadanie osiowosymetryczne). Analiza problemów tego typu ma istotne znaczenie w szeroko rozumianej mikrotechnologii i stąd wynika duże zainteresowanie badaniami teoretycznymi oraz eksperymentalnymi związanymi z ultraszybkim oddziaływaniem lasera na powierzchnię mikrowarstw wykonanych z różnych materiałów.

Przepływ ciepła w mikroskali może być opisany m.in. równaniem różniczkowym energii z dwoma czasami opóźnień (DPL – dual phase lag) i zgodnie z najnowszymi poglądami taki właśnie model stanowi najlepsze przybliżenie rzeczywistych procesów cieplnych zachodzących w tej skali. DPL wynika z uogólnienia znanego prawa Fouriera do którego wprowadza się dwa dodatkowe parametry τ_q i τ_T (czas relaksacji i czas termalizacji, odpowiednio).

Tematem rozważań w prezentowanej pracy jest model przepływu ciepła w jednorodnej warstewce materiału (chromu) poddanej działaniu zewnętrznego źródła ciepła (warunek brzegowy Neumanna) o zadanej zmiennej w czasie i na powierzchni intensywności q_b (funkcja typu dzwonowego, co implikuje orientację obiektu we współrzędnych walcowych), na pozostałych powierzchniach umownie ograniczających rozpatrywany obszar przyjęto warunki adiabatyczne.

Algorytm modelowania procesów cieplnych bazuje na jawnym schemacie MRS i w końcowej części pracy przedstawiono wyniki symulacji numerycznych.

Received: October 1, 2010
Received in a revised form: November 2, 2010
Accepted: November 8, 2010